VOLUME 6, NUMBER 6 • DECEMBER 2001 • ISSN 1087-0571

JOURNAL OF BIOMOLECULAR SCREENING

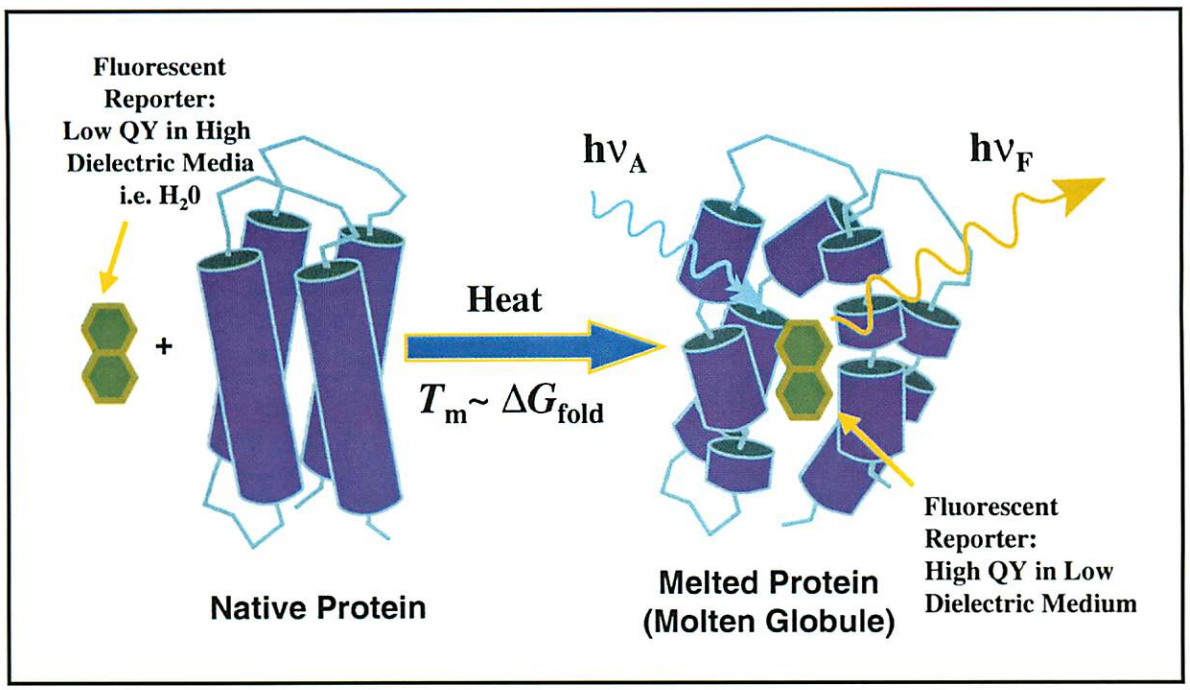

The Official Journal of The Society for Biomolecular Screening

Mary Ann Liebert, Inc. publishers

JOURNAL OF BIOMOLECULAR SCREENING
Volume 6, Number 6, 2001

High-Density Miniaturized Thermal Shift Assays as a General Strategy for Drug Discovery*

MICHAEL W. PANTOLIANO,† EUGENE C. PETRELLA, JOSEPH D. KWASNOSKI, VICTOR S. LOBANOV, JAMES MYSLIK, EDWARD GRAF, TED CARVER, ERIC ASEL, BARRY A. SPRINGER, PAMELA LANE, and F.R. SALEMME

ABSTRACT

More general and universally applicable drug discovery assay technologies are needed in order to keep pace with the recent advances in combinatorial chemistry and genomics-based target generation. Ligand-induced conformational stabilization of proteins is a well-understood phenomenon in which substrates, inhibitors, cofactors, and even other proteins provide enhanced stability to proteins on binding. This phenomenon is based on the energetic coupling of the ligand-binding and protein-melting reactions. In an attempt to harness these biophysical properties for drug discovery, fully automated instrumentation was designed and implemented to perform miniaturized fluorescence-based thermal shift assays in a microplate format for the high throughput screening of compound libraries. Validation of this process and instrumentation was achieved by investigating ligand binding to more than 100 protein targets. The general applicability of the thermal shift screening strategy was found to be an important advantage because it circumvents the need to design and retool new assays with each new therapeutic target. Moreover, the miniaturized thermal shift assay methodology does not require any prior knowledge of a therapeutic target's function, making it ideally suited for the quantitative high throughput drug screening and evaluation of targets derived from genomics.

INTRODUCTION

A MAJOR CHALLENGE CURRENTLY facing conventional high throughput screening drug discovery methodologies is the ability to rapidly judge relative binding affinities for the expanding numbers of new compounds derived from combinatorial chemical libraries. Compounding this task is the recent flood of new therapeutic targets that have become available from advances in genomics-based efforts in both human and microbial organisms. Moreover, many of the targets derived from genomics have unknown functions[1,2] and/or unknown *in vivo* ligands (i.e., orphan receptors),[3,4] making conventional assay development and drug screening problematic. Therefore, it has become increasingly apparent that more general and universally applicable assays are needed in order to scale with the exponential growth of diverse compounds and targets. Some examples of general assay strategies have begun to appear in the literature,[5] many of which employ electron spray mass spectrometry as the ligand-binding detection system.[6,7]

Thermal shift assays have many biophysical attributes that satisfy the requirements of a general cross-target drug discovery assay. Ligand-induced conformational stabilization of proteins is a well-understood phenomenon in which substrates, inhibitors, cofactors, metal ions, synthetic analogs of natural ligands, and even other proteins provide enhanced stability to proteins on binding.[8–11] This phenomenon is based on the energetic coupling of the ligand-binding and receptor-melting reactions, as depicted in Figure 1. This energetic linkage results in ligand-dependent changes in the midpoint for thermally induced melting curves for the ligand–receptor complex relative to the uncomplexed receptor (ΔT_m) that are directly proportional to the ligand binding affinity (K_a). Traditionally, thermal shift assays have been conducted using differential scanning calorimeters (DSCs) that monitor the change in heat capacity

3-Dimensional Pharmaceuticals, Inc., Exton, PA.
*Supported in part by Small Business Innovative Research (SBIR) Grant R43 GM52786 (Phases I & II, 1995–1998) from the National Institute of General Medical Sciences at the National Institutes of Health.
†Present address: Millennium Pharmaceuticals Inc., Cambridge, MA.

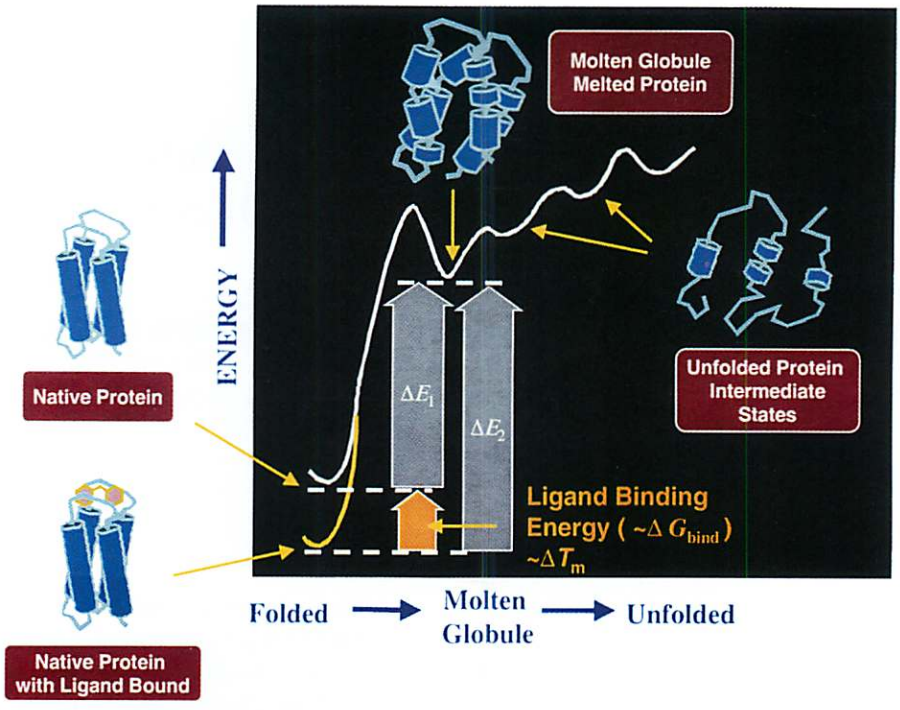

FIG. 1. Energetics of ligand-induced conformational stabilization of proteins. The energetics of thermal shift assays is based on ligand-dependent receptor stabilization, as monitored by ΔT_m measurements for the melting transitions of ligand–receptor complexes, relative to the uncomplexed receptor. This ligand–receptor stabilization is directly related to the ligand binding affinity (ΔG_{bind}) because of the thermodynamic linkage between the ligand–receptor binding and ligand–receptor melting free energy functions (ΔG_{bind} and ΔE_1, respectively). It is generally believed that the molten globule is the first state encountered during protein phase transitions[50–52] for most proteins, and the energetics depicted here reflect this phenomenology.

as proteins undergo temperature-induced melting transitions.[8,12] In addition, biophysical methods that employ temperature-regulated optical instrumentation that measures temperature-dependent changes in absorbance, fluorescence, and circular dichroism have also been historically used to perform thermal shift assays.[13–15]

In order to exploit the nearly universal physicochemical properties of ligand-induced stabilization of proteins for applications in drug discovery, we have miniaturized the thermal shift assay for use in a high-density microplate format. The validation of this miniaturized thermal shift process, along with the implementation of the instrumentation and software, is the subject of this report.

EXPERIMENTAL PROCEDURES

Proteins

The human α-estrogen receptor (ESR) was purchased from PanVera (Madison, WI). Bacteriorhodopsin (*H. halobium*) was purchased from Sigma Chemical Co. (St. Louis, MO). Human α-thrombin was purchased from Enzyme Research Labs (South Bend, IN). Bovine liver dihydrofolate reductase (DHFR) was purchased from Sigma. The extracellular domains of the fibroblast growth factor receptor-1 [D(II)-D(III) FGFR-1] were cloned from a human placenta library and expressed as a secreted protein from HEK293E cells (details to be described elsewhere). The PilD enzyme, a leader peptidase and an *N*-methyltransferase from *Pseudomonas aeruginosa*, was a generous gift from Wim Hol of the University of Washington (Seattle).

Fluorescent dyes

The environmentally sensitive dyes 1-anilinonaphthalene-8-sulfonic acid (1,8-ANS), 2,6-ANS, 2-(*p*-toluidinyl)-napthalene-6-sulfonic acid (2,6-TNS), and the 5-(4″-dimethylaminophenyl)-2-(4′-phenyl)oxazole family of dyes (Dapoxyl® sulfonic acid) were purchased from Molecular Probes (Eugene, OR). Environmentally sensitive dyes are fluorophores that have low quantum yields (low QY) in solvents with high dielectric constants, such as water, but are highly fluorescent (high QY) in solvents with low dielectric constants, such as ethanol and dioxane.[16] Examples of these dyes include the napthylamine sulfonic acids such as 1,8-ANS, 2,6-ANS, and 2,6-TNS, and also the Dapoxyl family of dyes.[17] They can be used as extrinsic probes of unfolded or melted proteins because the dyes partition themselves into the melted protein or molten globule states that have low dielectric properties resembling those of organic solvents. The result is a large increase in fluorescence for the extrinsic dye as a function of protein thermal melting. These dyes are excited in the near-ultraviolet region and have emission in the visible region (460–530 nm).

Microplate thermal shift assay process and instrumentation

The protein–dye solutions were first dispensed into each well of a 384-well microplate (polystyrene conical-well microplates; MJ Research, Inc., Waltham, MA) in equal 2.5- or 5.0-μL aliquots. Then an equal volume of test compound solution (typically 100–200 μM in 5%–10% DMSO) were dispensed into each well to yield test ligands at 50–100 μM in an assay volume of 5.0–10.0 μL. The resulting amount of protein utilized for an average therapeutic target is 0.25–0.50 μg/well (~1.5 μM for an ~30.0-kDa protein) or 100–200 μg/plate, depending on the volume chosen. Finally, a small volume of mineral oil was added to each well to eliminate evaporation. Reference control wells (no test ligands), containing the appropriate amount of DMSO, were distributed on the 384-well plate, usually in rows 12 and 24. The plates were subsequently heated in the custom-designed microplate thermal shift assay instrument (Fig. 2), which automatically monitored the complete thermal melting of the proteins through closed-circuit device (CCD) camera detection of changes in fluorescence for the extrinsic environmentally sensitive fluorophore. A Genesis 5000 liquid handling robot (Tecan Group Ltd., Männedorf, Switzerland) controlled the fluidics dispensing of all reagents to assay microplates.

RESULTS

Microplate thermal shift process and instrumentation

A fully automated miniaturized thermal shift assay that works in a high-density microplate format was designed and implemented so that 384 protein melting transitions are simultaneously processed. Pilot and beta instruments were con-

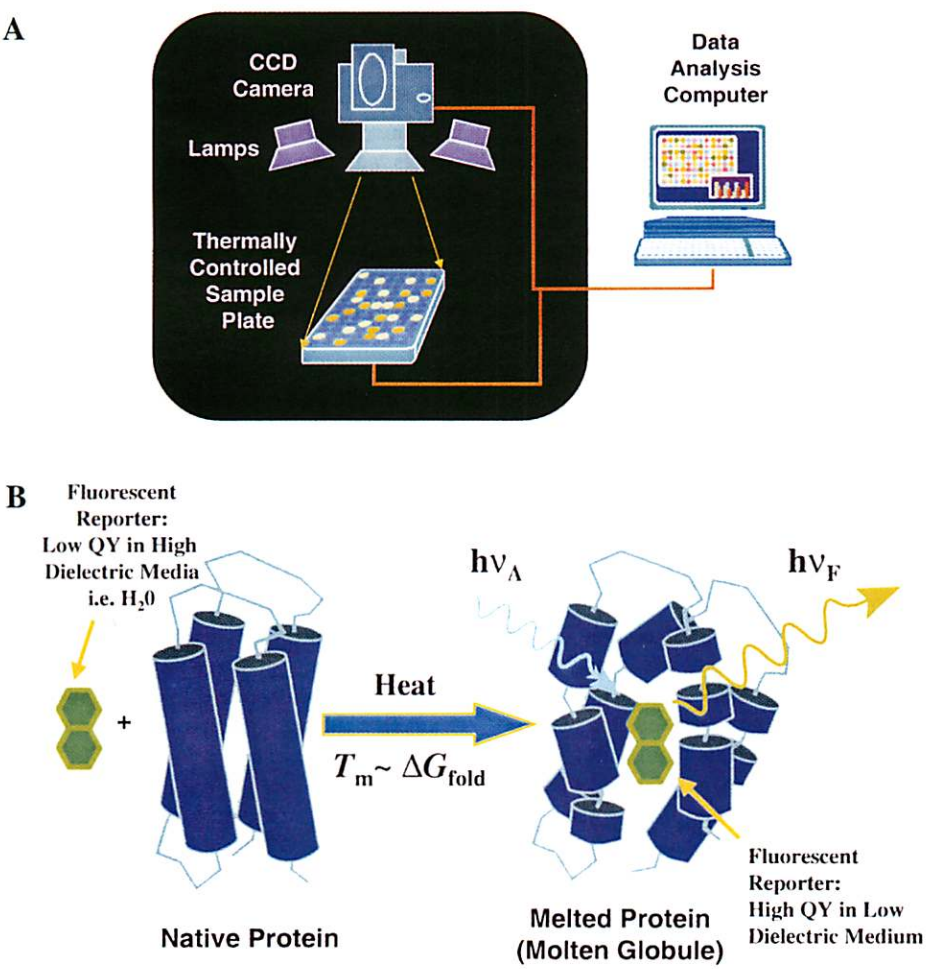

FIG. 2. (**A**) Microplate thermal shift instrumentation. The hardware employed for this study utilized a noncooled CCD imaging camera that automatically captured the fluorescence changes resulting from the extrinsic dyes that correspond to the thermal melting transitions of proteins as they were simultaneously heated on a computer-controlled heating block. Microplate heating occurred for 1- to 3-min intervals in 0.1° to 5.0°C increments for any temperature range between 25° and 99°C. The CCD images were collected at each designated time/temperature point and then stored on a personal computer for analysis at the end of the temperature range. Typically, microplate images were collected at 20–40 temperature points. Microplate well-to-well temperature uniformity was controlled to yield protein melting temperatures (T_m) with standard deviations that did not exceed ±0.25°C for all 384 wells in the absence of ligands. Epiillumination from long-wavelength ultraviolet lamps provided the excitation light, and a selectable band pass filter allowed the desired fluorescence emission wavelengths to reach the CCD camera. (**B**) Fluorescence-based detection of thermal phase transitions in proteins.

structed to perform ~384 assays in ~1.5 h or ~6,000 assays/day, and are described in the legend to Figure 2A.

The miniaturized thermal shift assay process begins with a purified therapeutic protein (~75% pure) sample at ~100 μg/mL in a suitable buffer near neutral pH. The protein solution is then made 100 μM in an environmentally sensitive fluorescent dye and dispensed into each well of a 384-well microplate in equal 2.5- or 5.0-μL aliquots. The monitoring of miniaturized thermal phase transitions was accomplished through the use of environmentally sensitive fluorescent dyes as depicted in Figure 2B. A more detailed description of the microplate thermal shift process, together with the attending hardware and software, is found in *Experimental Procedures* and elsewhere.[18–20]

Validation studies

Validation of this process and the instrumentation was attempted by investigating ligand binding to more than 100 model and therapeutic target proteins. The following subset was selected from these model systems to illustrate the utility of miniaturized thermal shift assays for diverse classes of proteins.

Nuclear hormone receptors: ESR. The nuclear hormone receptors are a superfamily of ligand-activated DNA-binding transcription factors. ESR is the prototype member of this class of receptors involved in the regulation of eucaryotic gene expression and affecting cellular proliferation and differentiation in target tissues.[21] This receptor is composed of several domains important for hormone binding,[22] DNA binding,[23] and activation of transcription.

The thermal melting transition for ESR was observed to be at 44.5°C in the absence of ligands, but was increased to 49.8°C in the presence of the known antagonist tamoxifen (Fig. 3A). Good agreement was found for the binding affinity measurement made by the miniaturized thermal shift assay (K_d = 1.1 μM) and that reported in the literature (IC_{50} = 0.42 μM).[24]

Often the pretransitional and posttransitional baselines (y_f and y_u, respectively) for the well containing the ligand do not match those for the control well. This discrepancy has three components: (1) optical effects, (2) liquid-handling variation, and (3) quenching of signal as a result of the ligand. The optical effects are derived from the limitations of using a CCD camera with epi-illumination. There are optical edge effects that result from the lens of the camera, and there are optical perspective effects caused by the depth of the wells so that the fluorescence measured for wells near the middle of the plate is larger than that measured near the edges. In addition, the epi-illumination yields variable excitation light across the plate, which results in variable emission. Nonuniformity across the CCD camera chip can also contribute to the observed variability in the pre- and posttransitional baselines. The liquid-handling variation introduces small differences in volumes of reagents that result in differences in observed absolute fluorescence intensity. Also, introduction of bubbles during reagent delivery will change the absolute fluorescence intensity derived from different wells. Some degree of quenching of the fluorescence signal derived from the environmentally sensitive dyes occurs for a subset of test compounds. However, the observed variations in absolute fluorescence signal are not a problem for these miniaturized thermal shift assays because both the pre- and posttransitional baselines (y_f and y_u) are measured independently for each well. Consequently, the critical thermal melting parameters, T_m and ΔH_u, for each well were also determined independently within the intrawell boundaries of y_f and y_u (see Eqn. 3 in the Appendix).

Growth factor and cytokine receptors: FGFR-1. The FGFR-1 extracellular domains, D(II)-D(III) FGFR-1, have been shown to be important for ligand-binding interactions.[25–27]* The known ligand pentosan polysulfate, a sulfated oligosaccharide, was found to increase the T_m by 2.5°C (Fig. 3B), which corresponds to a K_d of 5.5 μM at 25°C when calculated using Equation 3 (see Appendix). This is in good agreement with a reported K_d of 11 μM for this ligand measured using isothermal titration calorimetry.[27]

Integral membrane proteins. The utility of the miniaturized thermal shift assay strategy as a drug discovery tool for the integral membrane protein class was demonstrated with the following examples.

PilD from *Pseudomonas aeruginosa*. The enzyme PilD is a putative five-transmembrane enzyme with two catalytic activities, a leader peptidase and an *N*-methyltransferase activity, that are essential for the proper processing of the type IV pili proteins expressed on the surface of many gram-negative pathogens.[28,29] The results for the miniaturized thermal shift assay of ligands binding to PilD are shown in Figure 3C. The *N*-methyltransferase activity cofactor *S*-adenosyl-L-methionine was found to increase the T_m by 1.1°C, which corresponds to a binding affinity of K_d = 900 μM. This is in good agreement with the K_d of ~300 μM previously measured using a radioactive competition assay.[30]

Bacteriorhodopsin. The seven-transmembrane protein bacteriorhodopsin is a light-driven proton pump from bacterial purple membranes and is commonly used as a model for structure–function studies of G protein–coupled receptors (GPCRs).[31] The form of bacteriorhodopsin with retinal covalent binding to Lys 216 was reconstituted in nonionic detergents and investigated for its compatibility with the miniaturized thermal shift process. The melting transition for this receptor–ligand complex was observed to occur at 73.3°C, as shown in Figure 3D.

Screening of combinatorial libraries directed at the serine protease human α-thrombin. A series of seven focused combinatorial libraries directed against the catalytic site of the serine protease α-human thrombin were first assayed using a spectrophotometric enzyme assay* and then compared with results

*One of four different receptors, FGFR1 through FGFR4,[25] that bind fibroblast growth factors, a family of 18 related polypeptides, FGF1 through FGF18,[26] with broad mitogenic and cell survival activities. These receptors have been demonstrated to be important for embryonic development, angiogenesis, and wound healing in adults.

*The enzymatic assays employ spectrophotometric substrates such as succinyl-Ala-Ala-Pro-Arg-*p*-nitroanilide, which releases the colored product *p*-nitroanilide on hydrolysis.

*The enthalpy measurement in the miniaturized thermal shift assay is the equivalent of a Van't Hoff enthalpy determination.

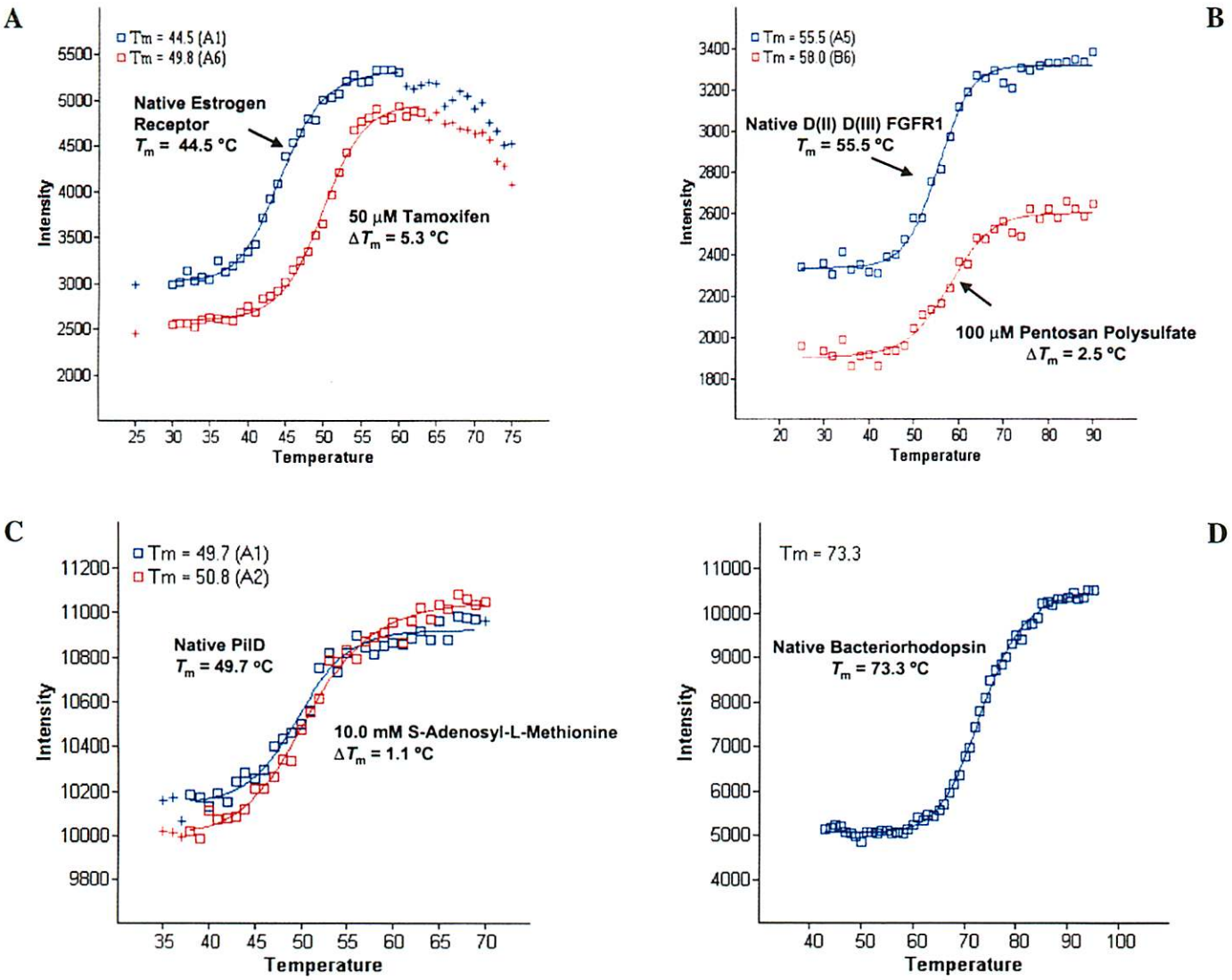

FIG. 3. Miniaturized thermal shift assay results for diverse classes of enzymes and receptors. (**A**) Ligand binding to the human α-estrogen receptor. The estrogen receptor was diluted into 50 mM Tris (pH 8.0), 80 mM KCl, 1.6% glycerol, 1.0 mM EDTA, 1.0 sodium vanandate, 2 mM dithiothreitol, and 10 mM $MgCl_2$ buffer, which also contained 100 μM of the fluorophore Dapoxyl sulfonic acid. Fluorescence intensity was measured as a function of temperature using the instrumentation described Figure 2. The known antagonist tamoxifen was present at 50 μM, and the final assay volume was 10.0 μL. The *solid lines* through each of the data sets were fit using Equation 1. The binding affinity (K_d) at 25°C was calculated using Equation 3 and was found to be 1.1 μM for tamoxifen. An IC_{50} of 0.42 μM for tamoxifen was previously measured by fluorescence polarization.[24] (**B**) Ligand binding to fibroblast growth factor receptor-1. Miniaturized thermal shift assay data were obtained for D(II)-D(III) FGFR-1 in the presence and absence of ligands. The midpoint for the unfolding transition in the absence of ligands was observed to be 55.5°C, while a known ligand, pentosan polysulfate, was observed to give a 2.5°C increase in T_m under the same conditions. The calculated K_d (at 25°C) was found to be 5.5 μM (Eqn. 3), which compares favorably with the K_d of 11 μM measured through isothermal titration calorimetry. The buffer conditions for the assays were 50 mM phosphate-buffered saline with 40 mM sodium citrate (pH 7.2), 10 mM $MgCl_2$, 2 mM EDTA, and 2% glycerol. (**C**). Ligand binding to the processing enzyme PilD, an example of an integral membrane protein. Miniaturized thermal shift assays were performed for PilD in the presence and absence of ligands. The melting transition in the absence of ligands (100 mM HEPES [pH 7.5] and 200 mM NaCl in 12.3 mM *n*-octyl-β-D-glucopyranoside [~0.5 CMC_{H2O}]) was observed to have a T_m of 49.7°C. The known ligand, *S*-adenosyl-L-methionine, (10.0 mM) is a cofactor for the methyl transferase activity of this enzyme, and was observed to give a 1.1°C increase in T_m. This corresponds to a calculated K_d of 900 mM at 25°C (Eqn. 3) and compares favorably with the K_d of 500 mM reported in the literature. The assays were performed as described above with 2 μg/well PilD. (**D**) Bacteriorhodopsin, an example of a seven-transmembrane protein. Miniaturized thermal shift assays were performed for the retinal-bound form of bacteriorhodopsin from *H. halobium*. The protein was solubilized in 5 mM NaOAc (pH 5.0) buffer containing 6.4 mM *n*-nonyl-β-D-glucopyranoside (~CMC_{H2O}). The melting transition for this retinal-bound covalent complex was observed to have a T_m of 73.3°C. The assays were performed as described above.

obtained using the miniaturized thermal shift process (Fig. 4). The seven focused libraries consisted of seven 96-well plates synthesized in sequential order. There were 213 hits out of the original 665 compounds with binding affinities that span ~3.5 orders of magnitude.

The results from the miniaturized thermal shift assay were found to correlate with the results obtained through the enzymatic assay as demonstrated by the reasonable fit to the slope = 1.0 line for the log/log plot. The deviation of the data from a perfect fit can come from a number of sources, the first of which is the time interval (~6 months) between the enzyme and thermal shift assays. Time-dependent changes for some labile ligands could account for some differences between the two methods. Another source of some of the deviation may come from the range of ligand-binding enthalpies (ΔH_L = 0.0 to −25.0 kcal/mol) one might expect for an assortment of different ligands binding to a given target. (For examples of compounds that have binding affinities that are entropically driven, see refs. 12 and 32.) This potential assortment for ligand-binding enthalpies translates into a range for the calculated K_a (at T) for any given ligand when estimated using Equation 3 (see Appendix). For example, the use of thrombin, a ligand that yields a ΔT_m of 2.0°C, results in a calculated K_a (at 37°C) of 8.5×10^5 when ΔH_L = 0.0 (Eqn. 3), while a ligand with ΔH_L = −25.0 kcal/mol yields a calculated K_a (at 37°C) of 7.1×10^6. Thus, in the case of thrombin, a 10-fold range in the estimated K_a is possible for a given value of ΔT_m, which is consistent with the observed variation in Figure 4. Finally, there could be a small subset of compounds that that interact with both the native and unfolded forms of thrombin, thereby resulting in smaller ΔT_m determinations (and smaller K_a) than expected if the ligand bound only to the native form of thrombin.

Data analysis for these screening experiments was simplified using a software interface that graphically displays the computed ΔT_m determinations for all 384 wells of the microplate thermal shift assay, as shown in Figure 5. The results for one of the library plates (Plate 6) screened against thrombin is shown using an adjustable-gradient color code for ΔT_m measured for each well—the more positive the ΔT_m for an individual compound, the more deeply red-shaded the well. White signifies little or no change in T_m compared with a control (T_0) in which no compounds are present. Thus hits can be visually identified and ranked by color and bar graph or, alternatively, they may be listed in tables that show the ΔT_m values and estimated binding affinities (K_a values) for all 384 wells (not shown). More details concerning the data analysis software tools are located in the Appendix.

The software interface that graphically displays the computed

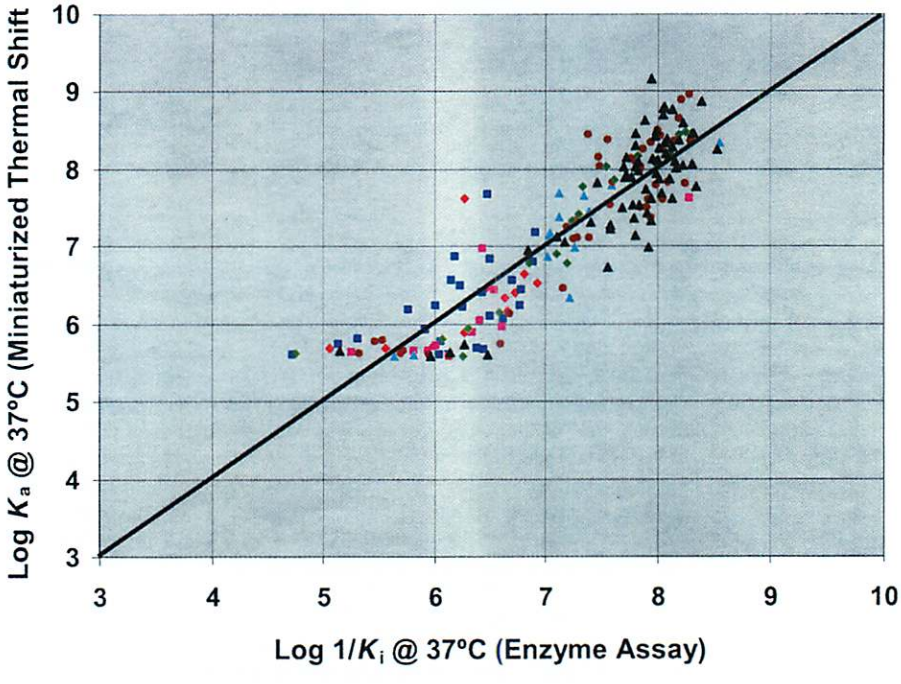

FIG. 4. Screening of focused combinatorial libraries directed at the catalytic site of human α-thrombin. Seven focused combinatorial libraries directed at the catalytic site of human thrombin were first assayed by a conventional enzymatic spectrophotometric assay and then compared with the results obtained using the miniaturized thermal shift process. The seven focused libraries consisted of seven 96-well plates (1 through 7) synthesized in sequential order: *red diamonds* = plate 1; *blue boxes* = plate 2; *magenta boxes* = plate 3; *cyan triangles* = plate 4; *brown circles* = plate 5; *green diamonds* = plate 6; *black triangles* = plate 7. The results were plotted in a log/log format for direct comparison of the extent to which the two different assay measurements are consistent. The *solid line* of slope 1.0 represents a perfect match for the two methods of analysis. Thrombin was present at 1.0 μM in 50 mM Hepes (pH 7.5) and 0.1 M NaCl, and the Dapoxyl sulfonic acid was present at 100 μM. Excitation of the fluorophore was effected using a long-wavelength ultraviolet lamp, and the emission was filtered through a band-pass filter that allowed 500- to 530-nm wavelength light to pass to the CCD camera. The compounds from the focused libraries were present at a final concentration of ~17 μM.

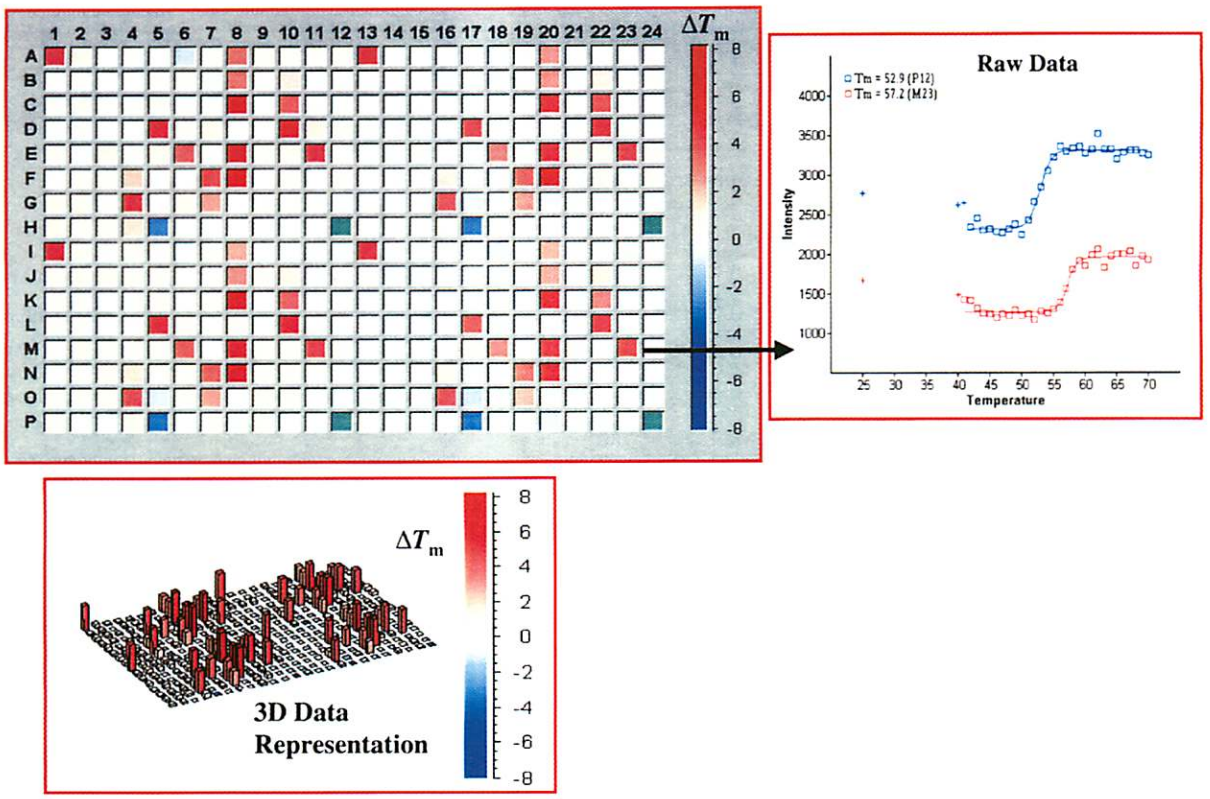

FIG. 5. Data analysis software tools. The ΔT_m data analysis for one of the seven compound library plates, plate 6, screened against human thrombin (Fig. 4) is shown in various levels of detail. The software used to analyze the miniaturized thermal shift assays performed in 384-well plates displays the ΔT_m values as an adjustable-gradient color code, shown at the right of the simulated 384-well plate. The more red the well, the more positive the ΔT_m. Similarly, the more blue the well, the more negative the ΔT_m. White signifies little or no change in T_m compared with control (T_0). The original 96-well plate of compounds was replicated four times on the 384-well assay plate in a quad format to reveal the level of reproducibility of these measurements (A1, A13, I1, and I13 have the identical compound). The control wells, which contain only DMSO, are designated as green, which for this plate are wells H12, H24, P12, and P24. The fluorescence intensity versus temperature data for any well can be displayed for demonstration purposes by double clicking on any well. An example is shown at the right for well M23, which is compared with the data for a control P12. This compound shows a ΔT_m of 4.3°C and is one of the 21 hits on this plate with ΔT_m 0.5°C. A three-dimensional bar chart representation of the ΔT_m data for this plate is also shown at the bottom. The software was written in C++ and runs on all Microsoft Windows™-based platforms.

ΔT_m determinations for all 384 wells of the microplate thermal shift assay is described in the legend to Figure 5.

Multiligand binding events. A demonstration of the effects of multiligand binding events on the miniaturized thermal shift assay appears in Table 1. Binding of the coenzyme $NADP^+$ and the folate mimetic methotrexate (MTX) to the bovine liver enzyme DHFR was analyzed individually as well as together. Alone, the individual ligands produced ΔT_m values of 6.3°C for $NADP^+$ and 7.7°C for MTX, which correspond to binding affinities of K_d = 2.4 μM for $NADP^+$ and 5.8 nM for MTX (at 25°C), when calculated using Equation 3. The measurement for MTX is in agreement with those appearing in the literature (see Table 1). Importantly, when both ligands are present together, there is a much larger increase in ΔT_m of 18.1°C, indicating that the ligand-induced stabilization is to some extent additive, although the observed shift is 4.1°C larger than that expected for the simple sum of the ΔT_m values for the individual ligands. This deviation from perfect additivity suggests some positive cooperativity for these two ligands binding at adjacent sites. Support for this supposition comes from the structural and functional evidence for positive cooperativity of the binding of these two ligands at adjacent sites in DHFR enzymes from both eukaryotic and prokaryotic organisms.[33–35] For example, a 100-fold increase in binding affinity of MTX (at 10°C) was reported when NADPH was bound to the bovine liver DHFR[36] (see Table 1).

DISCUSSION

General drug discovery applications

The successful measurements of binding affinity for assorted ligands binding to diverse classes of protein targets (Figs. 3 and 4) demonstrate that the miniaturized thermal shift assay strategy has wide cross-target utility. Of the ~100 protein–ligand complexes investigated to date, only proteins with heme groups

TABLE 1. EVALUATION OF MULTILIGAND BINDING USING MINIATURIZED THERMAL SHIFT ASSAYS: BOVINE LIVER DHFR AS A TEST CASE[a]

Ligand(s)	ΔT_m (°C)	K_d (nM)	K_d (nM) in literature
	Miniaturized Thermal Shift Data		
None	T_m = 51.8 ± 0.4	—	—
$NADP^+$ (10 mM)	6.3 ± 0.1	2400	No data
NADPH (10 mM)	9.7 ± 0.2	81.0	40 (human)[b]
MTX (0.1 mM)	7.7 ± 0.4	5.8	3.3[c]
$NADP^+$ & MTX	18.1 ± 0.4 (Σ = 14.0)	Positive cooperativity: ΔT_m = +4.1°C > Σ	Positive cooperativity: MTX binds 12.5-fold tighter (*E. coli*)[d]
NADPH & MTX	24.6 ± 0.6 (Σ = 17.4)	Positive cooperativity: ΔT_m = +7.2°C > Σ	Positive cooperativity: MTX binds 100-fold tighter (K_d = 0.033 nM)[c]
	DSC Data[e]		
None	T_m = 49.1	—	See ref. 35
NADPH	8.2	—	See ref. 35
MTX	13.3	—	See ref. 35
NADPH & MTX	29.0 (Σ = 21.5)	Positive cooperativity: ΔT_m = +7.5°C > Σ	See ref. 35

[a]The cooperativity of ligand binding to bovine liver DHFR was investigated using the miniaturized thermal shift assay. Conditions employed were 50 mM HEPES (pH 7.5) and 100 mM NaCl, in a volume of 5 μL. Σ = sum of individual ΔT_m values for two ligands when present alone (i.e., MTX and NADPH) under identical conditions.

[b]A K_d for NADPH binding to bovine liver DHFR could not be found; however, the K_d for the human enzyme was reported to be 40 nM by Schweitzer et al.[33]

[c]Gilli et al.[36] These conditions were for bovine liver DHFR at pH 6.8 (0.1 M potassium phosphate buffer) at 10°C.

[d]Cooperativity for $NADPH^+$ and MTX binding to *Escherichia coli* DHFR.[34]

[e]Differential scanning calorimetry (DSC) conditions employed by Sasso et al.[35] were pH 6.8 (0.1 M potassium phosphate buffer).

were observed to yield low fluorescence as a result of quenching of the extrinsic dye fluorescence signal, although this did not preclude using the assay at a higher concentration.

The binding affinity results obtained for the miniaturized thermal shift assay were found to be largely consistent with the results obtained through enzymatic, radioactive, fluorescence polarization, isothermal titration calorimetry, or other kinds of assays. This was best demonstrated by the correlation between the continuous spectrometric enzyme assay and thermal shift data for the combinatorial libraries directed at the catalytic site of thrombin (Fig. 4).

One advantage of the miniaturized thermal shift strategy is the fundamental biophysical basis of the assay, which circumvents the need to design and retool new assays for each new protein target. Another related outcome is that this strategy does not require any prior knowledge of a specific therapeutic target's function in order to screen libraries and optimize drug leads. In this regard, the results for bacteriorhodopsin and the estrogen receptor suggest that the miniaturized thermal shift assay strategy will be useful for drug discovery efforts with GPCRs and nuclear hormone receptors, especially those orphan receptors for which drug screening presents a problem because of the lack of known ligands. These properties make a miniaturized thermal shift assay strategy ideally suited for high throughput drug screening and evaluation of targets derived from genomics.

Multiligand binding applications

The data in Table 1 illustrate the utility of the miniaturized thermal shift assay for assessing multiligand binding to protein targets. The data show that this process can not only identify ligands binding to substrate binding sites of enzymes, but also identify and judge the cooperativity of ligands binding to cofactor, allosteric, and/or regulatory sites on therapeutic targets. Exosites on enzymes are often useful targets of therapeutic intervention, as demonstrated by the thrombin cofactor heparin, an effective anticoagulant.[37,38] In this regard, the miniaturized thermal shift assay could be used in conjunction with protein structural information (nuclear magnetic resonance [NMR] or x-ray diffraction), and be used to identify ligands binding at ad-

jacent sites (Table 1). In this application, the thermal shift assay may serve as an ideal source of information for structure-based drug design approaches such as the "SAR by NMR" approach first described by Shuker et al.[39]

The assessment of multiligand binding interactions illustrates an advantage that a thermal shift assay has over other assays that are often limited to a single binding site on a protein. The universal nature of the thermal assay extends to all potential ligand binding sites over the entire surface (and volume) of a protein molecule. Moreover, cooperativity (positive or negative) for ligand binding is quickly determined by the deviation from additivity for the ΔT_m measurements (see Table 1), and all at a single ligand concentration in a single well. Similarly, by eliminating the necessity for dose ranging of the ligand concentration, the thermal shift assay leads to a large dynamic range for assessing ligand binding affinity using a single ligand concentration.[8] Indeed, the results for ligand binding to thrombin (Fig. 4) illustrate that 3.5 orders of magnitude in binding affinity, corresponding to a ΔT_m range of 0.5° to ~10.0°C, can be assessed at a single ligand concentration (17 μM) and in single respective wells.

High throughput screening technical issues

Some technical issues that were observed while performing high throughput screening of large compound libraries (~100,000) included occasional fluorescence quenching of the extrinsic dyes by a small subset of library compounds. This can be minimized by adjusting the concentration of compounds to be screened so that they are ~25 μM or lower. This screening concentration will obviate the identification of hits with K_d greater than ~12 μM, but many of these weaker hits are often ignored anyway when more potent hits are present.

Another issue that was observed on occasion is related to the multiligand binding phenomenon discussed above. Compounds that can bind to more than one site on a protein will appear more potent because of the additivity of the ΔT_m values for the respective binding sites. Although this can be useful information, especially in the context of structure-based drug design, it can bias a structure–activity relationship analysis of hits. Dose ranging of initial hits can help to identify these multisite ligands because of the larger dependence of ΔT_m on the concentration of ligand expected for these compounds (see Eqn. 2 in Appendix). We also have employed isothermal titrating calorimetry[40] to obtain stoichiometry measurements for compounds with unusually large ΔT_m values.

The hit validation process for "positives" that come out of miniaturized thermal shift assay primary screens starts off very similar to those from other HTS assays in that families of compounds with different chemical scaffolds are chosen for dose ranging to estimate potency. However, because binding enthalpy can be different for different compound classes, some variability is introduced into the calculations for the apparent K_d for individual compounds. Thus, in the absence of any other secondary assay, it is necessary to give all classes even weight when it comes to potency until other properties and characteristics (i.e., liquid chromatography–mass spectrometry quality control) take their toll in winnowing down the number of classes of compounds still considered valid hits. Carrying three or more classes of compounds through hit validation programs is not uncommon anyway. For example, at many pharmaceutical companies, testing purified solids is often a point at which positives drop out of consideration because of the decay of compounds in liquid DMSO stocks, resulting in false positives (in any assay). Moreover, at the point at which one has purified solids, it is also possible to employ isothermal titration calorimetry to directly measure binding enthalpy and K_d for a few members of each lead series and reevaluate potency.

Finally, further improvements in liquid handling and instrumentation will enable additional miniaturization of the thermal shift assay to 1.0-μL and lower volumes, which will greatly reduce the amount of protein required per well (assay).

ACKNOWLEDGMENTS

Financial support in the form of Small Business Innovative Research (SBIR) Grant R43 GM52786 (Phases I & II, 1995–1998) from the National Institute of General Medical Sciences at the National Institutes of Health is gratefully acknowledged. We thank Wim Hol at the University of Washington (Seattle) for providing the PilD enzyme. We also thank Kannan Ramachandran for HTS assistance. Many useful discussions with A. W. Rhind and R. Bone concerning fluorescence imaging are also gratefully acknowledged.

REFERENCES

1. Tatusov RL, Koonin EV, Lipman DJ: A genomic perspective on protein families. *Science* 1997;278:631–637.
2. Koonin EV, Tatusov RL, Galperin MY: Beyond complete genomes: from sequence to structure and function. *Curr Opin Struct Biol* 1998;8:355–363.
3. Laudet V: Evolution of the nuclear receptor superfamily: early diversification from an ancestral orphan receptor. *J Mol Endocrinol* 1997;19:207–226.
4. Stadel JM, Wilson S, Bergsma DJ: Orphan G protein-coupled receptors: a neglected opportunity for pioneer drug discovery. *Trends Pharmacol Sci* 1997;18:430–437.
5. Eliseev A: Emerging approaches to target assisted screening of combinatorial mixtures. Curr Opin Drug Discov Dev 1998;1:106–115.
6. Zhao YZ, van Breemen RB, Nikolic D, et al: Screening solution-phase combinatorial libraries using pulsed ultrafiltration/electrospray mass spectrometry. *J Med Chem* 1997;40:4006–4012.
7. Chu YH, Dunayevskiy YM, Kirby DP, et al: Affinity capillary electrophoresis-mass spectrometry for screening combinatorial libraries. *J Am Chem Soc* 1996;118:7827–7835.
8. Brandts JF, Lin L: Study of strong to ultratight protein interactions using differential scanning calorimetry. *Biochemistry* 1990;29:6927–6940.
9. Schellman JA: Macromolecular binding. *Biopolymers* 1975;14: 999–1018.
10. Pace CN, McGrath T: Substrate stabilization of lysozyme to thermal and guanidine hydrochloride denaturation. *J Biol Chem* 1980;255:3862–3865.
11. Straume M, Friere E: Two-dimensional differential scanning

calorimetry simultaneous resolution of intrinsic protein structural energetics and ligand binding interactions by global linkage analysis. *Anal Biochem* 1992;203:259–268.
12. Weber PC, Pantoliano MW, Simons DM, et al: Structure based design of synthetic azobenzene ligands for streptavidin. *J Am Chem Soc* 1994;116:2717–2724.
13. Chavan AJ, Haley BE, Volkin DB, et al: Interaction of nucleotides with acidic fibroblast growth factor (FGF-1). *Biochemistry* 1994;33:7193–7202.
14. Morton A, Baase WA, Matthews BW: Energetic origins of specificity of ligand binding in an interior nonpolar cavity of T4 lysozyme. *Biochemistry* 1995;34:8564–8575.
15. Bouvier M, Wiley D: Importance of peptide amino and carboxyl termini to the stability of MHC class I molecules. *Science* 1994;265:398–402.
16. Lakowicz JR: *Principles of Fluorescence Spectroscopy.* New York: Plenum Press, 1983.
17. Diwu Z, Lu Y, Zhang C, et al: Fluorescent molecular probes II. The synthesis, spectral properties and use of fluorescent solvatochromic Dapoxyl dyes. *Photochem Photobiol* 1997;66:424–431.
18. Pantoliano MW, Rhind AW, Salemme FR, Springer BA, Bone R, Petrella EC: Microplate thermal shift assay and apparatus for ligand development and multi-variable protein chemistry optimization. International Patent Appl. No. PCT/US97/08154, Publ. No. WO 97/42500, 1997.
19. Pantoliano MW, Rhind AW, Salemme FR: Microplate thermal shift assay for ligand development and multi-variable protein chemistry optimization. US Patent 6,020,141 (Issued 2/1/2000).
20. Pantoliano MW, Bone RF, Rhind AW, et al: Microplate thermal shift assay apparatus for ligand development and multi-variable protein chemistry optimization. US Patent 6,036,920 (Issued 3/14/2000).
21. Brzozowski AJ. Pike AC, Dauter Z, et al: Molecular basis of agonism and antagonism in the oestrogen receptor. *Nature* 1997;389:753–758.
22. Tanenbaum DM, Wang Y, Williams SP, et al: Crystallographic comparison of the estrogen and progesterone receptor's[sic] ligand binding domain. *Proc Natl Acad Sci U S A* 1998;95: 5998–6003.
23. Schwabe JWR, Chapman L, Finch JT, et al: The crystal structure of the estrogen receptor DNA-binding domain bound to DNA: how receptors discriminate between their response elements. *Cell* 1993;75:567–578.
24. Bolger R, Wiese TE, Ervin K, et al: Rapid screening of environmental chemicals for estrogen receptor binding capacity. *Environ Health Perspect* 1998;106:551–557.
25. Jaye M, Schlessinger J, Dionne CA: Fibroblast growth factor receptor tyrosine kinases: molecular analysis and signal transduction. *Biochim Biophys Acta* 1992;1135:185–199.
26. Ohbayashi N, Hoshikawa M, Kimura S, et al: Structure and expression of the mRNA encoding a novel fibroblast growth factor, FGF-18. *J Biol Chem* 1998;272:18161–18164.
27. Pantoliano MW, Horlick RA, Springer B, et al: Multivalent ligand-receptor binding interactions in the fibroblast growth factor system produce a cooperative growth factor and heparin mechanism for receptor dimerization. *Biochemistry* 1994;33:10229–10248.
28. Strom MS, Lory S: Structure-function and biogenesis of the type IV pili. *Annu Rev Microbiol* 1993;47:565–596.
29. Strom MS, Lory S: Kinetics and sequence specificity of processing of prepilin by PilD, the type IV leader peptidase of *Pseudomonas aeruginosa*. *J Bacteriol* 1992;174:7345–7351.
30. Strom MS, Nunn DN, Lory S: A single bifunctional enzyme, PilD, catlyzes cleavage and N-methylation of proteins belonging to the type IV pilin family. *Proc Natl Acad Sci U S A* 1993;90:2404–2408.
31. Pebay-Peyroula E, Rummel G, Rosenbusch JP, et al: X-ray structure of bacteriorhodopsin at 2.5 angstoms from microcrystals grown in lipidic cubic phases. *Science* 1997;277:1676–1681.
32. Biltonen RL, Langerman N: Microcalorimetry for biological chemistry: experimental design, data analysis, and interpretation. *Methods Enzymol* 1979;61:287–319.
33. Schweitzer BI, Dicker AP, Bertino JR: Dihydrofolate reductase as a therapeutic target. *FASEB J* 1990;4:2441–2452.
34. Bystroff C, Kraut J: Crystal structure of unliganded *Escherichia coli* dihydrofolate reductase: ligand-induced conformational changes and cooperativity in binding. *Biochemistry* 1991;30:2227–2239.
35. Sasso S, Protasevich I, Gilli R, et al: Thermal denaturation of bacterial and bovine dihydrofolate reductases and their complexes with NADPH, trimethoprim and methotrexate. *J Biomol Struct Dyn* 1995;5:1023–1032.
36. Gilli RM, Sari JC, Lopez CL, et al: Comparative thermodynamic study of the interaction of some antifolates with dihydrofolate reductase. *Biochim Biophys Acta* 1990;1040:245–250.
37. Rosenberg RD, Bauer KA: In Coleman RW, Hirsh J, Marder VJ, et al. (eds): *Hemostasis and Thrombosis: Basic Principles and Clinical Practices,* 3rd ed. Philadelphia: JB Lippincott,1994:837–860
38. Lane DA, Bjork I, Lindahl U (eds): Heparin and related polysaccharides. *Adv Exp Med Biol* 1992;313.
39. Shuker SB, Hajduk PJ, Meadows RP, et al: Discovering high-affinity ligands for proteins: SAR by NMR. *Science* 1996;274:1531–1534.
40. Wiseman T, Williston S, Brandts JF, et al: Rapid measurement of binding constants and heats of binding using a new titration calorimeter. *Anal Biochem* 1989;179:131–137.
41. Schwarz FP, Puri K, Surolia A: Thermodynamics of the binding of galactopyranoside derivatives to the basic lectin from winged bean (*Phosphocarpus tetrogonolobus*). *J Biol Chem* 1991;266: 24344–24350.
42. Copeland RA, Ji H, Halfpenny AJ, et al: The structure of human acidic fibroblast growth factor and its interaction with heparin. *Arch Biochem Biophys* 1991;289:53–61.
43. Tsai PK, Volkin DB, Dabora JM, et al: Formulation designs of acidic fibroblast growth factor. *Pharm Res* 1993;10:649–659.
44. Volkin DB, Tsai PK, Dabora JM, et al: In Ladisch M, Bose A (eds): *Proceedings of the American Chemical Society Conference: Harnessing Biotechnology for the 21st Century.* Washington DC: American Chemical Society, 1992:298–302
45. Brandts JF, Hu CQ, Lin LN, et al: A simple model for proteins with interacting domains: applications to scanning calorimetry data. *Biochemistry* 1989;28:8588–8596.
46. Shrake A, Ross PD: Biphasic denaturation of human albumin due to ligand redistribution during unfolding. *J Biol Chem* 1988;263: 15392–15399.
47. Manly SP, Matthews KS, Sturtevant JM: Thermal denaturation of the core protein of lac repressor. *Biochemistry* 1985;24:3842–3846.
48. Edge V, Allewell NM, Sturtevant JM: High-resolution differential scanning calorimetric analysis of the subunits of *Escherichia coli* aspartate transcarbamoylase. *Biochemistry* 1985;24:5899–5906.
49. Sanchez Ruiz JM, Lopez-Lacomba JL, Mateo PL, et al: Analysis of the thermal unfolding of porcine procarboxypeptidase A and its functional pieces by differential scanning calorimetry. *Eur J Biochem* 1988;176:225–230.

50. Ptitsyn OB, Pain RH, Semisotnov GV, et al: Evidence for a molten globule state as a general intermediate in protein folding. *FEBS Lett* 1990;262:20–24.
51. Ptitsyn OB: Structures of folding intermediates. *Curr Opin Struct Biol* 1995;5:74–78.
52. Dobson CM: Protein folding: solid evidence for molten globules. *Curr Biol* 1994;4:636–640.

Address reprint requests to:
Michael W. Pantoliano
Millennium Pharmaceuticals, Inc.
270 Albany Street
Cambridge, MA 02139

E-mail: pantoliano@mpi.com

APPENDIX

Data analysis and software tools

A nonlinear least-squares fitting algorithm was used to fit the fluorescence imaging data collected by the CCD camera using the following expression:

$$y(T) = y_u + \frac{(y_f - y_u)}{1 + \exp\{-\Delta H_u/R[1/T - 1/T_m] + \Delta C_{pu}/R[\ln(T/T_m) + T_m/T - 1]\}} \quad (1)$$

where $y(T)$ is the fluorescence unfolding data as a function of T for each well in a 384-well plate, and the five fitting parameters, T_m, ΔH_u, ΔC_{pu}, y_f, and y_u, are allowed to float according to the Levenberg-Marquardt algorithm for minimizing the sum of the squares of the residuals. T_m is the midpoint for the protein unfolding transition, and $T_m = T_0$ in the absence of li-gands (control). ΔH_u is the protein unfolding enthalpy,* and $\Delta H_u = \Delta H_u{}^{T0}$ in the absence of ligands (control). ΔC_{pu} is the heat capacity change for protein unfolding, and $\Delta C_{pu} = \Delta C_{pu}{}^{T0}$, in the absence of ligands (control). The parameters y_f and y_u are the pretransitional and posttransitional fluorescence intensity levels, respectively.

The five fitting parameters for all 384 melting curves are then stored in a lookup table and a sixth parameter, the ΔT_m values for the test ligands, is then computed by subtracting the average T_0 value for the controls on the plate from the experimental T_m values for the ligands. Those test ligands that result in a ΔT_m value greater than a predetermined cutoff threshold, usually $\Delta T_m = +0.5$°C or greater, are identified as ligands binding to the target protein (i.e., a qualified hit). The software interface that graphically displays the computed ΔT_m determinations for all 384 wells of the microplate thermal shift assay is described in the legend to Figure 5.

Finally, a seventh parameter corresponding to the estimated ligand binding affinity, K_L^{Tm}, at T_m is calculated using the following expression, first described by Brandts and Lin[8]:

$$K_L^{Tm} = \frac{\exp\{-\Delta H_u{}^{T0}/R[1/T_m - 1/T_0] + \Delta C_{pu}{}^{T0}/R[\ln(T_m/T_0 + T_0/T_m - 1]\}}{[L_{Tm}]} \quad (2)$$

where

K_L^{Tm} = ligand association constant at T_m
T_m = midpoint for the protein unfolding transition in the presence of ligand
T_0 = midpoint for the unfolding transition in the absence of ligand
ΔH_u^{T0} = enthalpy of protein unfolding in the absence of li-gand at T_0
ΔC_{pu}^{T0} = change in heat capacity on protein unfolding in the absence of ligand
$[L_{Tm}]$ = free ligand concentration at T_m ($[L_{Tm}] \cong [L]_{total}$ when $[L]_{total} >> [Protein]_{total}$)
R = gas constant

To estimate the ligand binding affinity at any temperature (usually a reference temperature such as 25° or 37°C), it is necessary to use the additional expression:

$$K_L^T = K_L^{Tm} \exp\left\{-\frac{\Delta H_L^T}{R}\left[\frac{1}{T} - \frac{1}{T_m}\right] + \frac{\Delta C_{pL}^T}{R}\left[\ln\left(\frac{T}{T_m}\right) + 1 - \frac{T}{T_m}\right]\right\} \quad (3A)$$

where K_L^T is the protein/ligand binding association constant at any temperature T. The parameter ΔH_L^T is the ligand binding enthalpy, and the parameter ΔC_{pL}^T is the ligand heat capacity change on binding. The second exponential term in Equation 3A is nearly always very small, and reasonable approximations of K_L^T can be made using just the first exponential term, as shown in Equation 3B[9]:

$$K_L^T = K_L^{Tm} \exp\left\{-\frac{\Delta H_L^T}{R}\left[\frac{1}{T} - \frac{1}{T_m}\right]\right\} \quad (3B)$$

Therefore, the ligand binding enthalpy, ΔH_L^T, is the only parameter in Equation 3 not experimentally determined from the thermal melting transitions. For the majority of ligand/protein binding enthalpy measurements reported in the literature, however, an average near -10.0 to -15.0 kcal/mol[32,40] has been observed. In the absence of any other information, $\Delta H_L^T = -15.0$ kcal/mol can be used in Equation 3 to make reasonable estimates of K_L^T (see *Results*). T_m is the midpoint for the protein unfolding transition in the presence of ligand. K_L^{Tm} is the protein/ligand association constant at T_m (i.e., Eqn. 2). The values for T_0, ΔH_u^{T0} and ΔC_{pu} used in Equations 2 and 3 are derived from the fits for the unfolding curves (Eqn. 1) in the absence of ligands (i.e., reference wells on each plate).

Theory and practice for ligand-induced conformational stabilization of proteins

Nearly all proteins investigated to date (~100 unique proteins) by the miniaturized thermal shift methodology have yielded thermal melting transitions that are irreversible under the conditions employed. This is a common observation even for conventional thermal shift assays regardless of whether the measurements are made using DSC[8,41] or optical instrumentation.[42–44] The irreversible nature of thermal shift assays and the use of thermodynamic models to derive K_a values from those data (Eqn. 2 and 3) have been discussed at some length in the literature.[41,45,46] It has been argued that an overall irreversible unfolding process may be treated as a reversible unfolding reaction if the irreversible process (aggregation) of the unfolded species is slow compared with the rates of interconversion between the native and unfolded species.[47–49] Moreover, the reasonable correlation of binding affinities measured by thermal shift assays with those measured by other methods suggests that thermodynamic models adequately describe the majority of cases tested (both here and elsewhere[8,41]) despite the irreversible nature of thermal protein melting. For example, the results in Figure 4 provide a convincing argument that a diverse set of ~700 combinatorial compounds can be plausibly accessed for their relative binding affinities for thrombin using the miniaturized thermal shift process, notwithstanding the observed irreversible thermal melting of thrombin.

An additional caution is the multidomain nature of many proteins, which may not always be expected to follow a simple two-state mechanism for protein melting. Deviations from simple two-state unfolding mechanisms could lead to errors in estimating binding affinities from thermodynamic models for treating thermal shift assay data. This is something to be mindful of when approaching each new target. However, many multidomain proteins, indeed all of the ones studied here, often have domains that are sufficiently coupled energetically that they melt in a cooperative manner, yielding sharp two-state melting transitions. Again, the case of thrombin (and the other examples chosen for this study) illustrates the utility of using a simple two-state thermodynamic model for a multidomain protein (Fig. 4). Additional and more sophisticated models may be needed in the future to fit more complex data sets from miniaturized thermal shift assays, especially for those proteins that are not tightly coupled energetically.